Asian Journal of Chemistry; Vol. 31, No. 6 (2019), 1332-1342

ASIAN JOURNAL OF CHEMISTRY

https://doi.org/10.14233/ajchem.2019.21928

A Combined Experimental (FT-IR) and Computational Studies of 9-Chloroanthracene

KATTAESWAR SRIKANTH[1,†], RAMAIAH KONAKANCHI[2,†] and JYOTHI PRASHANTH[3,*]

[1]Department of Physics, D.N.R. College (A), Bhimavaram-534204, India
[2]Department of Chemistry, National Institute of Technology, Warangal-506004, India
[3]Department of Physics, Kakatiya University, Warangal-506009, India
†These authors are equal contribution.

*Corresponding author: E-mail: prashanthjyothi2009@gmail.com

Received: 9 January 2019; *Accepted*: 7 March 2019; *Published online*: 29 April 2019; AJC-19377

The experimental FT-IR spectral analysis of 9-chloroanthracene has worked out by using density functional theory (DFT). The optimized molecular structure and minimum energy of 9-chloroanthracene has analyzed using DFT/B3LYP functional employing 6-311++G(d,p) basis set. The vibrational frequencies along with IR intensities were computed, scaling was used for a better fit between the experimental and computed frequencies, they agreed with rms error 8.48 cm^{-1} for 9-chloroanthracene. The NLO behaviour of the molecule is investigated from first-order hyperpolarizability. The HOMO and LUMO energies are evaluated to demonstrate the chemical stability, reactivity of molecule. The MESP over the molecules were plotted to evaluate electron density regions and thermodynamic parameters are calculated. Hyper conjugative interactions and charge delocalization of the molecule study from NBO analysis and Fukui functions are evaluated for 9-chloroanthracene. The molecular docking studies were performed against anticancer protein targets Tyrosinase and HER2.

Keywords: 9-Chloroanthracene, Vibrational analysis, First order hyperpolarizability, NBO analysis, Molecular docking.

INTRODUCTION

Anthracene having a molecular formula $C_{14}H_{10}$ containing three fused benzene rings and comes under polycyclic aromatic hydrocarbon (PAH). Anthracene and its derivatives are used in many research areas due to its many applications arising from various spectroscopic properties and chemical reactivity. They are generally used as probes in fluorescence [1-5]. They are also used as a labeling in biological systems [6], bio imaging [7,8] and significant biological and medicinal activity [9]. Pseudo urea is a drug containing anthracene used in clinical testing trials [10]. Anthracyclines are used as a treatment of cancer which inhibits the base pairs of the DNA/RNA results preventing the reproduction of rapidly-growing cancer cells [11]. Sidman [12] reported electronic and vibrational states of anthracene using the polarized absorption and fluorescence spectra. Vibrational and electronic spectral analysis using experimental and DFT approach of 9-anthracene methanol was investigated by Kou *et al.* [13]. The crystallographic studies and intermolecular hydrogen bonding transformations of 1-chloroanthracene and its photodimer were investigated by Turowska-Tyrk and Grzesniak [14]. To the best of our knowledge, the complete vibrational analysis and its quantum chemical characteristics of 9-chloroanthracene was not been reported in the admissible task so far. Keeping in view of the literature, we investigated experimental and theoretical calculations on the vibrational spectra of 9-chloroanthracene with the help of FT-IR and density functional theory (DFT) calculations. The molecular characteristics *i.e.* polarizability, first-order hyperpolarizability and dipole moment to calculate the NLO behaviour. MESP, thermodynamic parameters and HOMO-LUMO energies are calculated. To make the NBO analysis to study the stability of the molecules rising from hyper conjugative interactions and charge delocalization. Further, *in silico* docking studies were performed against 3pp0 and 3nm8 are target proteins by using Autodock.

EXPERIMENTAL

9-Chloroanthracene is purchased from Sigma-Aldrich and used as such without further purification. For IR spectral measurements, the spectra were recorded over the range of 4000-450 cm^{-1} using Perkin Elmer spectrum RX1 spectrometer.

Computational details: The computations were established by using the standard density functional triply-parameter hybrid model DFT/B3LYP [15] employing 6-311++G(d,p) basis set (*i.e.* the valence triple basis set, augmented by d polarization functions on carbon and nitrogen atoms, p polarization functions on hydrogen atoms and enlarged by diffuse functions on all atoms). *In silico* molecular docking studies have been performed by employing Auto Dock 4.2 package suite and Auto Dock Tools (ADT) (http://mgltools.scripps.edu) version 1.5.6 [16]. Visualize the ligand and receptor interactions by Discover Studio Visualizer 4.0 software [17].

RESULTS AND DISCUSSION

Molecular geometry: The most optimized molecular structure of 9-chloroanthracene has obtained from density functional theory employing with B3LYP/6-311++G(d,p) basis set using the Gaussian09W, as presented along with numbering in Fig. 1. The geometrical parameters bond distances, bond angles and dihedral angles of 9-chloroanthracene were reported in Table-1. The geometric parameters are in good agreement with experimental counters parts [14]. From DFT calculations, the average calculated value of aromatic C–C bond lengths in anthracene ring of 9-chloroanthracene is found to be 1.406 Å, which is in good agreement with single crystal XRD value 1.395 Å. The average theoretical value of aromatic ∠CCC bond angle of anthracene ring is found to be 119.9 Å, which is good agreement with those of experimental value 120.0 Å. The average values of C-H bond distances and ∠CCH bond angles of anthracene ring was computed as 1.083 and 119.44 Å,

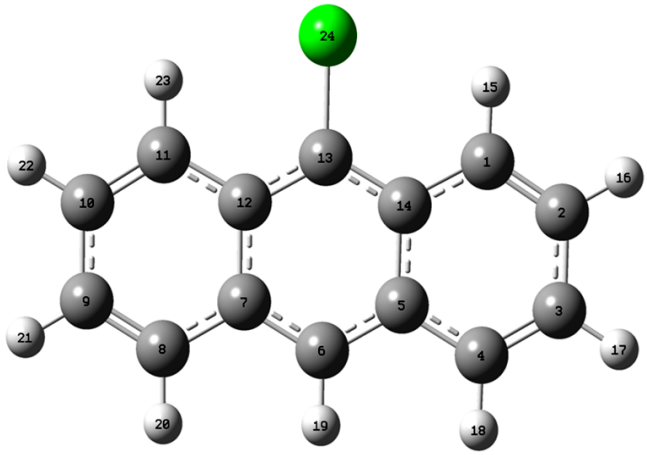

Fig. 1. Optimized molecular structure along with numbering of atoms for 9-chloroanthracene (E = -999.28020393 Hartree)

which are in good agreement with experimental value 0.95 and 119.50 Å obtained from X-ray studies.The bond distances (C-Cl) and bond angle (∠CCCl) between chlorine and anthracene ring are computed as1.765 and 118.46 Å, which are well agreement with experimental values 1.728 and 118.61 Å [14].

Vibrational analysis: The vibrational modes of the molecule under investigation is made using the DFT method employing B3LYP/6-311++G(d,p) basis set. 9-Chloroanthracene is composed of 24 atoms consists of 66 fundamental vibrations. They are dispensed as 45 in-plane vibrations and 21 out-of-plane vibrations of a-species in C_1 symmetry. To make a comp-

TABLE-1
OPTIMIZED GEOMETRICAL PARAMETERS OF 9-CHLOROANTHRACENE OBTAINED BY B3LYP/6-311++G(d, p) DENSITY FUNCTIONAL CALCULATIONS

Bond length	Value (Å)	Bond angle	Value (°)	Dihedral angle	Value (°)
C1-C2	1.367	C1-C2-C3	120.88	C1-C2-C3-C4	0.0
C2-C3	1.422	C2-C3-C4	119.99	C2-C3-C4-C5	0.0
C3-C4	1.365	C3-C4-C5	121.17	C3-C4-C5-C6	0.0
C4-C5	1.428	C4-C5-C14	118.79	C4-C5-C14-C1	0.0
C5-C14	1.444	C5-C14-C1	118.14	C5-C14-C1-C2	0.0
C14-C1	1.428	C14-C1-C2	121.00	C14-C1-C2-C3	0.0
C5-C6	1.395	C5-C6-C7	121.75	C5-C6-C7-C12	0.0
C6-C7	1.395	C6-C7-C12	119.75	C6-C7-C12-C13	0.0
C7-C12	1.444	C7-C12-C13	117.83	C7-C12-C13-C14	0.0
C12-C13	1.405	C12-C13-C14	123.06	C12-C13-C14-C5	0.0
C13-C14	1.405	C13-C14-C5	117.84	C13-C14-C5-C6	0.0
C7-C8	1.428	C14-C5-C6	119.75	C14-C5-C6-C7	0.0
C8-C9	1.365	C7-C8-C9	121.17	C7-C8-C9-C10	0.0
C9-C10	1.422	C8-C9-C10	119.99	C8-C9-C10-C11	0.0
C10-C11	1.367	C9-C10-C11	120.88	C9-C10-C11-C12	0.0
C11-C12	1.428	C10-C11-C12	121.00	C10-C11-C12-C7	0.0
C1-H15	1.081	C11-C12-C7	118.14	C11-C12-C7-C8	0.0
C2-H16	1.084	C12-C7-C8	118.79	C12-C7-C8-C9	0.0
C3-H17	1.084	C14-C1-H15	118.88	C5-C14-C1-H15	-180.0
C4-H18	1.084	C1-C2-H16	119.67	C14-C1-C2-H16	-180.0
C6-H19	1.085	C2-C3-H17	119.65	C1-C2-C3-H17	180.0
C8-C20	1.084	C3-C4-H18	120.61	C2-C3-C4-H18	180.0
C9-H21	1.084	C5-C6-H19	119.12	C14-C5-C6-H19	-180.0
C10-H22	1.084	C7-C8-H20	118.20	C12-C7-C8-H20	-180.0
C11-H23	1.081	C8-C9-H21	120.35	C7-C8-C9-H21	-180.0
C13-Cl24	1.765	C9-C10-H22	119.43	C8-C9-C10-H22	180.0
		C10-C11-H23	120.11	C9-C10-C11-C23	-180.0
		C12-C13-Cl24	118.46	C7-C12-C13-Cl24	-180.0

lete explanation of vibrations by normal coordinate analysis. For this motivation, the full set of 96 primitive (or standard) internal valence coordinates was defined as represents in Table-2. By an acceptable linear combination of these internal coordinates, a non-redundant set of 66 natural internal coordinates was established ensuing the guidance of Fogarasi *et al*. [18,19]. These are depicted in Table-3. The theoretically calculated DFT force field was transformed into natural symmetry coordinates, by using Molvib.7.0 program, normal coordinate was performed on 9-chloroanthracene [20,21]. According to the scaled quantum mechanical procedure, scaling of force constants was made [22,23] using selective scaling in the natural coordinate representation [18,24]. This is required to offset the systematic errors [25]. The complete vibrational assignments of fundamental modes of the molecule along with computed IR intensities and normal mode established characterized by PED are presented in Table-4. The root mean square (rms) deviation between the calculated and experimental frequencies was obtained emplo-

TABLE-2
DEFINITION OF INTERNAL COORDINATES OF 9-CHLOROANTHRACENE

S. No	Symbol	Type	Definition
		Stretching	
1-16	d_i	C-C (aromatic)	C1-C2, C2-C3, C3-C4, C4-C5, C5-C14, C14-C1, C5-C6, C6-C7, C7-C12, C12-C13, C13-C14, C7-C8, C8-C9, C9-C10, C10-C11, C11-C12
17-25	r_i	C-H (aromatic)	C1-H15, C2-H16, C3-H17, C4-H18, C6-H19, C8-H20, C9-H21, C10-H22, C11-H23
26	r_i	C-Cl	C13-Cl24
		Bending	
27-44	θ_i	C-C-C (aromatic)	C1-C2-C3, C2-C3-C4, C3-C4-C5, C4-C5-C14, C5-C14-C1, C14-C1-C2, C5-C6-C7, C6-C7-C12, C7-C12-C13, C12-C13-C14, C13-C14-C5, C14-C5-C6, C7-C8-C9, C8-C9-C10, C9-C10-C11, C10-C11-C12, C11-C12-C7, C12-C7-C8
45-62	β_i	C-C-H (aromatic)	C14-C1-H15, C2-C1-H15, C1-C2-H16, C3-C2-H16, C2-C3-H17, C4-C3-H17, C3-C4-H18, C5-C4-H18, C5-C6-H19, C7-C6-H19, C7-C8-H20, C9-C8-H20, C8-C9-H21, C10-C9-H21, C9-C10-H22, C11-C10-H23, C10-C11-H23, C12-C11-H23
63-64	β_i	C-C-Cl	C12-C13-Cl24, C14-C13-Cl24
		Out-of-plane bending	
65-82	δ_i	C-C-C-C	C1-C2-C3-C4, C2-C3-C4-C5, C3-C4-C5-C14, C4-C5-C14-C1, C5-C14-C1-C2, C14-C1-C2-C3, C5-C6-C7-C12, C6-C7-C12-C13, C7-C12-C13-C14, C12-C13-C14-C5, C13-C14-C5-C6, C14-C5-C6-C7, C7-C8-C9-C10, C8-C9-C10-C11, C9-C10-C11-C12, C10-C11-C12-C7, C11-C12-C7-C8, C12-C7-C8-C9
83-91	γ_i	H-C-C-C	H15-C1-C14-C2, H16-C2-C1-C3, H17-C3-C2-C4, H18-C4-C3-C5, H19-C6-C5-C7, H20-C8-C7-C9, H21-C9-C8-C10, H22-C10-C9-C11, H23-C1-C10-C12
92	γ_i	Cl-C-C-C	Cl24-C13-C12-C14
93-96	τ_i	C-C-C-C (butterfly)	C13-C14-C5-C4, C1-C14-C5-C6, C11-C12-C7-C6, C13-C12-C7-C8

TABLE-3
SYMMETRY COORDINATES FOR IN-PLANE AND OUT-OF-PLANE VIBRATIONS OF 9-CHLOROANTHRACENE

S. No.	Type[a]	Definition[b]
1-16	ν(C-C) (ring)	d_1, d_2, d_3, d_4, d_5, d_6, d_7, d_8, d_9, d_{10}, d_{11}, d_{12}, d_{13}, $d_{14,}$ d_{15}, d_{16}
17-25	ν(C-H) (ring)	r_2, r_3, r_4, r_5, r_6, r_7, r_8, r_9, r_{10}
26	ν(C-Cl)	r_1
27-35	β(CCC) (ring)	$\theta_1-\theta_2+\theta_3-\theta_4+\theta_5-\theta_6/\sqrt{6}$, $2\theta_1-\theta_2-\theta_3+2\theta_4-\theta_5-\theta_6/\sqrt{12}$-$\theta_2+\theta_3-\theta_5+\theta_6/\sqrt{2}$, $\theta_7-\theta_8+\theta_9-\theta_{10}+\theta_{11}-\theta_{12}/\sqrt{6}$, $2\theta_7-\theta_8-\theta_9+2\theta_{10}-\theta_{11}-\theta_{12}/\sqrt{12}$, $-\theta_8+\theta_9-\theta_{11}+\theta_{12}/\sqrt{2}$, $\theta_{13}-\theta_{14}+\theta_{15}-\theta_{16}+\theta_{17}-\theta_{18}/\sqrt{6}$, $2\theta_{13}-\theta_{14}-\theta_{15}+2\theta_{16}-\theta_{17}-\theta_{18}/\sqrt{12}$, $-\theta_{14}+\theta_{15}-\theta_{17}+\theta_{18}/\sqrt{2}$
36-44	β(CH)	$\beta_3-\beta_4/\sqrt{2}$, $\beta_5-\beta_6/\sqrt{2}$, $\beta_7-\beta_8/\sqrt{2}$, $\beta_9-\beta_{10}/\sqrt{2}$, $\beta_{11}-\beta_{12}/\sqrt{2}$, $\beta_{13}-\beta_{14}/\sqrt{2}$, $\beta_{15}-\beta_{16}/\sqrt{2}$, $\beta_{17}-\beta_{18}/\sqrt{2}$, $\beta_{19}-\beta_{20}/\sqrt{2}$
45	β(CCl)	$\beta_1-\beta_2/\sqrt{2}$,
46-54	τ(CCCC)	$\delta_1-\delta_2+\delta_3-\delta_4+\delta_5-\delta_6/\sqrt{6}$, $-\delta_1+2\delta_2-\delta_3-\delta_4+2\delta_5-\delta_6/\sqrt{12}$, $\delta_1-\delta_3+\delta_4-\delta_6/2$, $\delta_7-\delta_8+\delta_9-\delta_{10}+\delta_{11}-\delta_6/\sqrt{6}$,$-\delta_7+2\delta_8-\delta_9-\delta_{10}+2\delta_{11}-\delta_{12}/\sqrt{12}$, $\delta_7-\delta_9+\delta_{10}-\delta_{12}/2$, $\delta_{13}-\delta_{14}+\delta_{15}-\delta_{16}+\delta_{17}-\delta_{18}/\sqrt{6}$, $-\delta_{13}+2\delta_{14}-\delta_{15}-\delta_{16}+2\delta_{17}-\delta_{18}/\sqrt{12}$, $\delta_{13}-\delta_{15}+\delta_{16}-\delta_{18}/2$
55-63	π(CH)	γ_2, γ_3, γ_4, γ_5, γ_6, γ_7, γ_8, γ_9, γ_{10}
64	π(CCl)	γ_1
65-66	Butterfly	$\tau_1-\tau_2/\sqrt{2}$, $\tau_3-\tau_4/\sqrt{2}$

[a]The symbols are used for description of the normal modes by PED in Table-4. [b]The internal coordinates used here are defined in Table-2.

TABLE-4
ASSIGNMENTS OF FUNDAMENTAL VIBRATIONS OF 9-CHLOROANTHRACENE BY NORMAL MODE ANALYSIS BASED ON SQM FORCE FIELD CALCULATIONS USING B3LYP/6-311++G(d,p)

S. No.	Mode[a]	Observed frequency (cm^{-1})	Calculated frequency (cm^{-1})		IR[b] (I_i)	PED (%) among types of Internal coordinates[c]
			Unscaled	Scaled		
1	ν(C-C)	1660	1687	1665	9.320	ν(C-C)(69), β(CH)(19)
2	ν(C-C)	1649	1678	1648	0.878	ν(C-C)(67), β(CH)(16), β(CCC)(10)
3	ν(C-C)	1621	1634	1624	1.409	ν(C-C)(69), β(CH)(18)
4	ν(C-C)	1595	1602	1593	5.698	ν(C-C)(74), β(CH)(11), β(CCC)(10)
5	ν(C-C)	1577	1584	1576	4.593	ν(C-C)(75), β(CH)(14)

6	ν(C-C)	1485	1497	1491	3.592	ν(C-C)(47), β(CH)(36), β(CCC)(14)
7	ν(C-C)	1440	1437	1432	1.642	ν(C-C)(85), β(CCC)(8)
8	ν(C-C)	1398	1415	1408	0.033	ν(C-C)(64), β(CH)(33)
9	ν(C-C)	1359	1363	1355	43.623	ν(C-C)(58), β(CH)(21), β(CCC)(14)
10	ν(C-C)	1339	1345	1354	36.539	ν(C-C)(60), β(CH)(22), β(CCC)(12)
11	ν(C-C)	1287	1296	1298	12.873	ν(C-C)(74), β(CH)(22)
12	ν(C-C)	1478	1495	1480	0.652	ν(C-C)(49), β(CH)(29), β(CCC)(15)
13	ν(C-C)	1422	1428	1412	6.950	ν(C-C)(76), β(CH)(22)
14	ν(C-C)	1523	1532	1519	3.592	ν(C-C)(78), β(CH)(20)
15	ν(C-C)	962	965	959	0.001	ν(C-C)(43), β(CH)(22), β(CCC)(17)
16	ν(C-C)	920	935	933	0.082	ν(C-C)(51), β(CH)(20), β(CCC)(19)
17	ν(C-Cl)	–	418	425	2.873	ν(C-Cl)(34), ν(C-C)(33), β(CCC)(17)
18	ν(C-H)	3015	3181	3017	1.737	ν(C-H)(99)
19	ν(C-H)	3023	3183	3020	0.026	ν(C-H)(99)
20	ν(C-H)	3027	3185	3022	8.292	ν(C-H)(98)
21	ν(C-H)	3032	3195	3031	3.715	ν(C-H)(99)
22	ν(C-H)	3035	3195	3032	51.141	ν(C-H)(100)
23	ν(C-H)	3046	3209	3045	78.093	ν(C-H)(99)
24	ν(C-H)	3048	3210	3046	18.348	ν(C-H)(98)
25	ν(C-H)	3063	3236	3070	17.348	ν(C-H)(99)
26	ν(C-H)	3067	3237	3071	5.656	ν(C-H)(100)
27	β(CCC)	675	681	681	2.571	β(CCC)(65), ν(C-C)(25)
28	β(CCC)	647	654	653	5.442	β(CCC)(85), ν(C-C)(11)
29	β(CCC)	–	642	630	11.621	β(CCC)(68), ν(C-C)(19)
30	β(CCC)	618	620	613	10.662	β(CCC)(83), ν(C-C)(12)
31	β(CCC)	–	510	505	9.213	β(CCC)(66), ν(C-Cl)(18), ν(C-C)(10)
32	β(CCC)	560	564	548	0.307	β(CCC)(75), β(CCl)(15)
33	β(CCC)	414	418	407	0.054	β(CCC)(75), ν(C-C)(13)
34	β(CCC)	392	389	389	0.044	β(CCC)(59), ν(C-C)(28)
35	β(CCC)	–	234	230	3.847	β(CCC)(64), ν(C-C)(25)
36	β(CCl)	–	239	234	0.330	β(CCl)(80), β(CCC)(11)
37	β(CH)	1041	1049	1044	1.982	β(CH)(49), ν(C-C)(49)
38	β(CH)	1135	1137	1134	9.957	β(CH)(59), ν(C-C)(39)
39	β(CH)	–	1050	1045	2.107	β(CH)(51), ν(C-C)(45)
40	β(CH)	1307	1304	1301	26.846	β(CH)(53), β(CCC)(28), ν(C-C)(17)
41	β(CH)	1265	1262	1252	0.959	β(CH)(46), ν(C-C)(45)
42	β(CH)	1214	1217	1206	0.577	β(CH)(62), ν(C-C)(31)
43	β(CH)	1206	1207	1193	0.594	β(CH)(81), ν(C-C)(14)
44	β(CH)	1178	1183	1170	0.919	β(CH)(64), ν(C-C)(34)
45	β(CH)	1185	1187	1180	1.756	β(CH)(74), ν(C-C)(19)
46	π(CH)	–	962	958	0.035	π(CH)(87), τ(CCCC)(11)
47	π(CH)	939	943	935	4.265	π(CH)(91)
48	π(CH)	887	907	885	20.956	π(CH)(63), τ(CCCC)(31)
49	π(CH)	870	872	862	0.012	π(CH)(93)
50	π(CH)	852	860	846	16.292	π(CH)(87), τ(CCCC)(12)
51	π(CH)	–	864	850	0.017	π(CH)(77), τ(CCCC)(15)
52	π(CH)	839	837	838	29.905	π(CH)(78), τ(CCCC)(11)
53	π(CH)	751	753	735	100.0	π(CH)(91)
54	π(CH)	754	753	753	0.001	π(CH)(91)
55	π(CCl)	–	131	126	0.268	π(CCl)(29), Butterfly(29), τ(CCCC)(18)
56	τ(CCCC)	796	790	794	7.713	τ(CCCC)(67) π(CH)(26)
57	τ(CCCC)	773	775	764	0.025	τ(CCCC)(72), π(CH)(18)
58	τ(CCCC)	597	599	602	0.729	τ(CCCC)(66), π(CH)(17), π(CCl)(11)
59	τ(CCCC)	538	554	538	1.451	τ(CCCC)(43), Butterfly(28), π(CCl)(20)
60	τ(CCCC)	495	506	496	0.064	τ(CCCC)(83), π(CH)(17)
61	τ(CCCC)	474	486	475	0.014	τ(CCCC)(51), Butterfly(30), π(CH)(18)
62	τ(CCCC)	400	403	398	2.709	τ(CCCC)(72), π(CH)(17)
63	τ(CCCC)	–	299	290	0.044	τ(CCCC)(74), π(CCl)(13)
64	τ(CCCC)	–	117	114	0.005	τ(CCCC)(90)
65	Butterfly	–	237	233	0.001	τ(CCCC)(44), Butterfly(33), π(CH)(20)
66	Butterfly	–	80	79	1.176	Butterfly(40), τ(CCCC)(28), π(CH)(16)

[a]Abbreviations: ν, stretching; β, in plane bending; π, out of plane bending; τ, torsion. [b]Relative infrared intensities are normalized to 100.
[c]Number in the parenthesis is % of PED and number before the parenthesis is vibrational mode. PED less than 10 % is not shown.

ying the equation given below, in sequence to get the goodness of fit.

$$rms = \sqrt{\left(\frac{1}{n-1}\right)\sum_{i=1}^{n}\left[(\nu_i)^{cal} - (\nu_i)^{exp}\right]^2}$$

where, $(\nu_i)^{cal}$ is the i^{th} calculated frequency, $(\nu_i)^{exp}$ is the i^{th} experimental frequency and 'n' is the number of experimental frequencies.

The rms error between unscaled frequencies and observed frequencies obtained with DFT/B3LYP/6-311++G(d,p) basis set for 9-chloroanthracene was found as 52.3 cm^{-1}. On using the refined scaling factors obtained from least-squares optimization technique, this deviation was reduced to 8.48 cm^{-1}. The theoretically FT-IR spectra are more well-ordered than the observed ones, since as many vibrations giving in gas phase leads to well built perturbation of infrared intensities of many other modes. For a visual analogy, the experimental and simulated FT-IR spectrum of 9-chloroanthracene is presented in Fig. 2.

Vibrational assignments: All the in-plane and out-of-plane vibrational assignments were made by mentioning to potential energy distribution (PED), Eigen vectors obtained in the computations. The results presented in Table-4 are self-explanatory.

Vibrations of anthracene ring: In 9-chloroanthracene, sixteen C-C stretching vibrations belongs to anthracene ring. The sixteen observed frequencies at 1660, 1649, 1621, 1595, 1577, 1523, 1485, 1478, 1440, 1422, 1398, 1359, 1339, 1287, 962 and 920 cm^{-1}, respectively could be identified from the spectra of IR. IR spectrum shows two strong bands at 1621 and 1440 cm^{-1}. The observed frequencies are well comparable with the calculated frequencies at 1665, 1648, 1624, 1593, 1576, 1519, 1491, 1480, 1432, 1412, 1408, 1355, 1354, 1298, 959 and 933 cm^{-1}, respectively. These vibrations are well accord with literature values [26].

In general, the absorption around 3100-3000 cm^{-1} corresponds to the C–H stretching vibrations. In the 9-chloroanthracene nine C-H stretching vibrations are observed. These vibrational modes are pure do not mix with any other vibrations having PED in the extent 99-100 %. Hence the bands observed at 3067, 3063, 3048, 3046, 3035, 3032, 3027, 3023 and 3015 cm^{-1}, respectively are identified and assigned as C–H stretching modes. They are well agreeable with the theoretical values at 3071, 3070, 3046, 3045, 3032, 3031, 3022, 3020 and 3017 cm^{-1}, respectively. The results are shown in Table-4. The bond observed in the range 1300-1020 cm^{-1} corresponds to C–H in-plane bending modes of benzene and its derivatives. The compound 9-chloroanthracene have nine C–H in-plane bending vibrations, are calculated at 1301, 1252, 1206, 1193, 1180, 1170, 1134, 1045 and 1044 cm^{-1}. These are well comparable and assigned to the observed frequencies at 1307, 1265, 1214, 1206, 1185, 1178, 1135 and 1041 cm^{-1}, respectively.

9-Chloroanthracene has nine ring in-plane bending vibrations which are substituent sensitive modes those falls in the spectral region of 681-230 cm^{-1}. Theoretically these modes are calculated at 681, 653, 630, 613, 505, 548, 407, 389 and 230 cm^{-1}, respectively. Experimentally these modes are obtained in the range 675-392 cm^{-1} with a considerable extent of potential energy distribution. These bending vibrations are well agreement with bands obtained in FT-IR spectrum and literature values [27,28] predicted in Table-4.

The nine CH out-of-plane bending vibrations of anthracene ring in 9-chloroanthracene are computed at 958, 935, 885, 862, 850, 846, 838, 753, 735 cm^{-1}, respectively from the PED distribution as a dominating contribution. Experimentally the modes are predicted at 939, 887, 870, 852, 839 and 751 cm^{-1}, respectively, out of which two are strong in IR absorption spectrum. The two frequencies, which are not observed could be predicted as 958 and 850 cm^{-1}.

In 9-chloroanthracene, nine ring torsions belong to anthracene ring are computed at 794, 764, 602, 538, 496, 475, 398, 290, 114 cm^{-1}. The ring torsion vibrations are obtained in the spectral range 796-400 cm^{-1} in the FT–IT spectrum of the titled compound based on the PED obtained in DFT computations. The two butterfly vibrational characters of the anthracene ring of 9-chloroanthracene are calculated at 233 and 79 cm^{-1} in the present work. The vibrational assignments made in the present calculations corresponding to anthracene ring of 9-chloroanthracene are in good agreement with literature for the related molecules [28-31].

C–Cl vibrations: The chlorine group of 9-chloroanthracene has three vibrations out of which two are in-plane vibrations and one out of plane vibration. The band near 234 and 425 cm^{-1} are computed as C-Cl stretching and βCCl in-plane bending vibrations with 34 and 80 % maximum PED character. The out-of-plane vibration πCCl is calculated at 126 cm^{-1} with 29 % of PED in the molecule under investigation using DFT studies, which fundamentals are well accord with literature values [32,33].

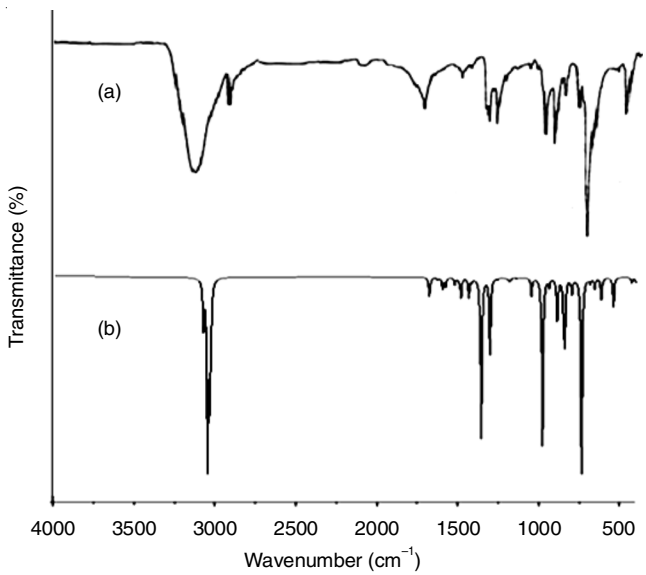

Fig. 2. (a) Experimental (b) simulated FT-IR spectra of 9-chloroanthracene

Frontier molecular orbitals: The chemical reactivity and kinetic stability of 9-chloroanthracene was distinguished with the assist of the frontier molecular orbital gap. A molecule with a lower frontier orbital gap is generally related to chemical reactivity and low kinetic stability [34,35]. The LUMO is an electron acceptor and HOMO is an electron donor. The frontier molecular orbitals gap is predicted the HOMO and LUMO orbital energies, the ionization energy (I), electron affinity (A),

global hardness (η), chemical potential (μ) and global electrophilicity power (ω) [36,37] of a molecule can be calculated as:

$$I = -E_{HOMO};\ A = -E_{LUMO};\ \eta = (-E_{HOMO} + E_{LUMO})/2;$$
$$\mu = (E_{HOMO}+E_{LUMO})/2;\ \text{and}\ \omega = \mu^2/2\eta.$$

The frontier molecular orbital and its parameters of 9-chloroanthracene are represented in Fig. 3 and Table-5. The calculated energy value of HOMO and LUMO energies of 9-chloroanthracene is -5.80012 and -2.35002 eV in the gas phase. The energy gap of the molecule under study is +3.45010 eV. The frontier energy gap of 9-chloroanthracene is very small posses negative chemical potential, which characters represents that the compound under study is stable and polarizable.

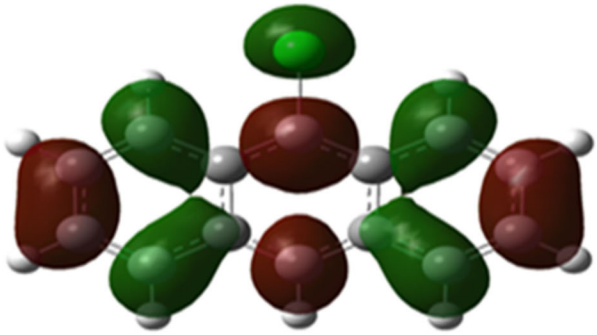

E_{LUMO} = –2.35002 eV

ΔE = 3.45040 eV

E_{HOMO} = –5.80012 eV

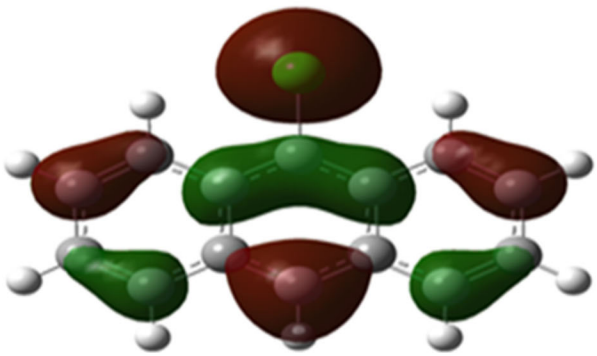

Fig. 3. Atomic orbital components of the Frontier molecular orbital of 9-chloroanthracene

TABLE-5
FRONTIER MOLECULAR ORBITAL
PARAMETERS OF 9-CHLOROANTHRACENE

Frontier molecular orbital parameter	9-Chloroanthracene (eV)
HOMO energy	-5.80012
LUMO energy	-2.35002
Frontier molecular orbital energy gap	3.45010
Ionization energy (I)	5.80012
Electron affinity (A)	2.35002
Global hardness (η)	1.72505
Chemical potential (μ)	-4.07507
Global electrophilicity power (ω)	4.81325

NLO properties: Density functional theory is an important tool to investigate the NLO properties of the organic and Inorganic compounds. The NLO property can be understood with the help of quantum chemical calculations [38,39]. The reaction of a compound in the applied field was described by the polarizability (α), total dipolemoment (μ_t) and hyperpolarizability (β) [40].

The electronic moments of a molecular system playa keyrole in structural chemistry. When a molecule with changeless electric dipole moment $\mu_e(0)$ interacts with an external constant electrostatic field E, the change in the dipole moment μ_t can be represented in tensor notation as:

The first order hyperpolarizability is a third rank tensor, which has 27 components, characterized by a 3 × 3 × 3 matrix. These 27 components get diminished to 10 components due to Klienman symmetry [41], which are shown as β_{xxx}, β_{xxy}, β_{xyy}, β_{yyy}, β_{xxz}, β_{xyz}, β_{yyz}, β_{xzz}, β_{yzz} and β_{zzz}. They can be resolved using the following equation [42].

$$\beta_i = \beta_{iii} + (1/3)\ \Sigma_{i\neq j}(\beta_{ijj} + \beta_{jij} + \beta_{jji})$$

The isotropic linear polarizability (α_t), the anisotropy of polarizability (Δα), the mean first order hyperpolarizability (β_t) and total static dipole moment (μ_t) using the x, y, z components are determined as:

$$\alpha_t = (\alpha_{xx} + \alpha_{yy} + \alpha_{zz})/3$$

$$\Delta\alpha = 2^{-1/2}\ [(\alpha_{xx} - \alpha_{yy})^2 + (\alpha_{yy} - \alpha_{zz})^2 + (\alpha_{zz} - \alpha_{xx})^2 + 6\alpha_{xx}^2\ ]^{1/2}$$

$$\beta_t = (\beta_x^2 + \beta_y^2 + \beta_z^2)^{1/2}$$

$$\mu_t = (\mu_x^2 + \mu_y^2 + \mu_z^2)^{1/2}$$

Hence, these properties like dipole moment (μ_t), polarizability (α) and first orderhyper polarizability (β) of the molecular system was calculated theoretically by DFT/B3LYP/6-311++G (d,p) method. The calculated values were tabulated in Table-6.

TABLE-6
VALUES OF DIPOLE MOMENT (μ_t, Debye)
AND FIRST ORDER HYPERPOLARIZABILITY
(β_t, 10^{-30} cm^5/e.s.u) OF 9-CHLOROANTHRACENE

Type of component	9-Chloro-anthracene	Type of component	9-Chloro-anthracene
β_{xxx}	-0.0334329	μ_x	-0.0001
β_{xxy}	-7.7628773	μ_y	-1.7181
β_{xyy}	-0.0179101	μ_z	0.000000
β_{yyy}	-213.7890413	μ_t	1.71730
β_{xxz}	0.000000	α_{xx}	272.650291
β_{xyz}	0.000000	α_{xy}	0.0015014
β_{yyz}	0.000000	α_{yy}	175.7401699
β_{xzz}	0.0002168	α_{xz}	0.000000
β_{yzz}	1.4034897	α_{yz}	0.000000
β_{zzz}	0.000000	α_{zz}	49.2952288
β_t	220.13 au (or) 1.901×10^{-30}esu	α_t	107.31533
		Δα	193.98947

We compared these results with urea, which is a prototypical material and used as a reference compound for comparative purposes. Generally these calculated values are in atomic units (a.u), so we have been converted into electrostatic units (esu) (α: 1 a.u. = 0.1482 × 10^{-24} esu, β: 1 a.u. = 8.6393 × 10^{-33} esu). The mean first order hyperpolarizability (β_t) 0.3728 × 10^{-30}cm^5/

esu and the total molecular dipole moment (μ_t) 1.3732 Debye of urea are used frequently as threshold values for the purpose of comparison. The total molecular dipole moment of the investigated compound was 1.71730 Debye and polarizability (α) was 107.31533 a.u. Further, the first order hyper polarizability (β_{tot}) was 1.901×10^{-30} cm^5/esu it is greater than the threshold value of urea, which reveals that the compound 9-chloroanthracene may be treated as better NLO applications.

Molecular electrostatic potential (MEP): MEP investigation gives information about the electrophilic and nucleophilic sites in a reaction and also shows that the hydrogen bonding interactions. The molecular electrostatic potential V(r) is mainly related to the electron density in a molecule. In order to know the MEP values in a molecule the following expression is used:

$$V(r) = \sum_A \frac{Z_A}{|R_A - r|} - \int \frac{\rho(r')}{|r' - r|} dr'$$

Here, N represents the total number of nuclei, Z_A represents the charge of the nucleus placed at R_A, $\rho(r')$ represents electron density function of the molecule and r′ is the dummy integration variable. The net resultant electrostatic effect V(r) is produced at the point r, by both the electrons and nuclei of the molecule, which can be determined either computationally or experimentally by diffraction methods [43-45].

Further to know the positive, negative and neutral electrostatic potential areas of the molecule under studied, MEP was calculated by using DFT. The MEP mapping of the investigated compound represented in the Fig. 4. The various values of electrostatic potential are represented by different colours; *i.e.* green, red, blue and yellow. These colours represent the region of zero potential, the maximum negative regions of electrostatic potential, positive electrostatic potential and slight electron negative. Potential increase in the order red < yellow < green < blue [46,47]. Any region at there has no electrostatic potential and it would be represented by green colour. The various regions at the surface of the molecule, which denotes electrophilic and nucleophilic regions are shown in red and blue colour respectively. The MEP of 9-chloroanthracene was shown in Fig. 4 observed that the region around aromatic carbon atoms of anthracene ring has a negative electrostatic potential region and the region around the Cl atom has positive electrostatic potential. Which convey that negative potential region is electrophilic and positive region potential region is nucleophilic for 9-chloroanthracene.

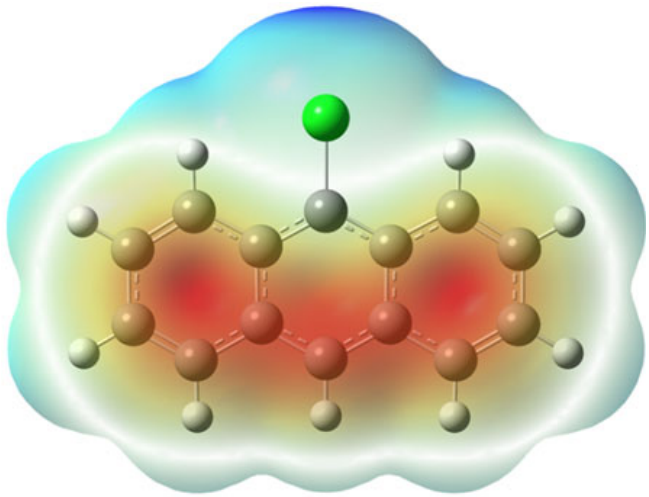

Fig. 4. B3LYP/6-311++G(d,p) calculated molecular electrostatic potential map of 9-chloroanthracene

Natural bond orbital analysis (NBO): The NBO investigation is an excellent tool for determining intra/inters molecular bonding and interactions with in the molecule. It gives useful information about interactions in both filled and virtual orbital spaces [48]. It is also valuable for determining the chemical interpretation of hyper conjugative interactions and electron density transfer from filled lone pair orbital of one subsystem and vacant orbital of another subsystem. The second order fock matrix has used to predict the interactions between the donor and acceptor orbitals in NBO investigation. For each donor (i) and acceptor (j), the stabilization energy $E^{(2)}$ associated with the delocalization i→j is estimated [49,50] as:

$$E(2) = -n_\sigma \frac{\langle \sigma | F | \sigma \rangle^2}{\varepsilon_\sigma^* - \varepsilon_\sigma} - n_\sigma \frac{F_{ij}^2}{\Delta E}$$

where, ε_σ^* and ε_σ are the energies of σ and σ^* NBOs, n_σ is the population of donor σ orbital and $\langle \sigma | F | \sigma \rangle^2$ is the Fock matrix element i and j NBO orbitals.

In this article, we have investigated the important electron donor orbital and electron acceptor orbital and the corresponding interacting stabilizing energies of 9-chloroanthracene. The NBO analysis was carried out to the molecular system by DFT/B3LYP/6-311+G(d,p) method and the results are presented in Table-7. The interaction between π (C12-C13) with antibonding π^*(C6-C7) is very much strong with the stabilization energy 228.11 kJ/mol, which also shows the strongest conju-

TABLE-7
SECOND ORDER PERTURBATION THEORY ANALYSIS OF FOCK MATRIX IN NBO BASIS FOR 9-CHLOROANTHRACENE

Donor(i)	Type	Ed/e	Acceptor(j)	Type	Ed/e	E(2)[a]	E(i)-E(j)[b]	f(I, j)[c]
C1-C2	σ	1.98172	C13-C14	σ*	1.97589	2.87	1.28	0.054
C1-C2	π	1.77066	C3-C4	π*	1.77607	16.29	0.30	0.069
	π		C5-C14	π*	1.50280	14.51	0.29	0.062
C1-C14	σ	1.97269	C1-C2	σ*	1.98172	2.58	1.30	0.052
	σ		C2-H16	σ*	1.98211	2.66	1.12	0.049
	σ		C5-C14	σ*	1.95821	3.22	1.21	0.056
	σ		C13-C14	σ*	1.97589	3.46	1.24	0.058
C1-H15	σ	1.98011	C2-C3	σ*	1.97934	4.07	1.05	0.058
	σ		C5-C14	σ*	1.95821	4.12	1.06	0.059
C2-C3	σ	1.97934	C4-H18	σ*	1.98075	2.91	1.12	0.051
C2-H16	σ	1.98211	C1-C14	σ*	1.97269	4.40	1.05	0.061
	σ		C3-C4	σ*	1.98200	3.19	1.14	0.033

C3-C4	σ	1.98200	C4-C5	σ*	1.97363	2.72	1.25	0.052
C3-C4	π	1.77607	C1-C2	π*	1.77066	15.92	0.30	0.062
	π		C5-C14	π*	1.50280	14.55	0.29	0.063
C3-H17	σ	1.98226	C4-C5	σ*	1.97363	4.31	1.05	0.060
C4-C5	σ	1.97363	C5-C6	σ*	1.97565	3.19	1.25	0.056
	σ		C5-C14	σ*	1.95821	3.06	1.21	0.054
C4-H18	σ	1.98075	C2-C3	σ*	1.97934	4.02	1.06	0.058
	σ		C5-C14	σ*	1.95821	4.19	1.06	0.060
C5-C6	σ	1.97565	C4-C5	σ*	1.97363	3.16	1.23	0.056
	σ		C5-C14	σ*	1.95821	3.51	1.24	0.059
C5-C14	σ	1.95821	C13-C14	σ*	1.97589	4.01	1.24	0.063
	σ		C13-Cl14	σ*	1.98877	4.70	0.81	0.055
C5-C14	π	1.50280	C1-C2	π*	1.77066	14.26	0.28	0.061
	π		C3-C4	π*	1.77607	14.07	0.28	0.061
	π		C6-C7	π*	1.61906	18.53	0.27	0.066
	π		C12-C13	π*	1.64593	19.99	0.26	0.065
C6-C7	σ	1.97565	C7-C12	σ*	1.95821	3.52	1.24	0.059
C6-C7	π	1.61906	C5-C14	π*	1.50280	19.76	0.28	0.068
	π		C8-C9	π*	1.77607	17.68	0.29	0.067
	π		C12-C13	π*	1.97588	19.87	0.27	0.066
C6-H19	σ	1.98040	C5-C14	σ*	1.95821	4.51	1.06	0.062
C7-C8	σ	1.97363	C6-C7	σ*	1.97565	3.19	1.25	0.044
C7-C12	σ	1.95821	C12-C13	σ*	1.97588	4.01	1.24	0.063
	σ		C13-Cl24	σ*	1.98877	4.70	0.81	0.055
C8-C9	π	1.77607	C6-C7	π*	1.61906	16.74	0.29	0.065
	π		C10-C11	π*	1.98172	15.92	0.30	0.062
C10-C11	π	1.77066	C8-C9	π*	1.77607	16.29	0.30	0.063
	π		C12-C13	π*	1.64593	18.30	0.28	0.067
C12-C13	π	1.64593	C5-C14	π*	1.50280	18.99	0.29	0.070
	π		C6-C7	π*	1.61906	16.07	0.030	0.062
	π		C10-C11	π*	1.77066	15.42	0.031	0.064
C5-C14	π	1.50280	C1-C2	π*	1.77066	180.52	0.01	0.076
	π		C3-C4	π*	1.77607	212.96	0.01	0.076
C12-C13	π		C6-C7	π*	1.61906	228.11	0.01	0.080

[a]E(2) means energy of hyper conjugative interaction(stabilization energy); [b]Energy difference between donor and acceptor i and j NBO orbitals; [c]$F(_{i,j})$ is the Fock matrix element between i and j NBO orbitals.

gation energy within the molecule. A strong interaction is observed between π (C5-C14) and the antibonding with π*(C1-C2) and π*(C3-C4) with a strong delocalization energy 180.52 kJ/mol and 212.96 kJ/mol, respectively. The interaction between σ (C1-C14) with antibonding σ* (C1-C2) and (C2-H16) has the delocalization energy 2.58 and 2.66 kJ/mol respectively which shows the lowest stabilization energy within the molecule. A moderate interaction is observed between π C5-C14 to the antibonding π* (C1-C2), π* (C3-C4), π* (C6-C7) and π* (C12-C13) with a hyper conjugation energy 14.26, 14.07, 18.53 and 19.99 kJ/mol, respectively.

Thermodynamic parameters: The standard thermodynamic functions such as SCF energy, zero-point energy (E_0), rotational constants (A, B and C), vibrational energy (E_{vib}), specific heat capacity at constant volume (C_v) and entropy (S) are calculated employing rigid rotor harmonic oscillator estimation using standard expressions [51,52] and with DFT using B3LYP/6-311++G(d,p) level of theory, reported in Table-8. The rotational constants A, B and C are calculated as 0.96181, 0.45037 and 0.30674 GHz.

TABLE-8
THERMODYNAMIC PARAMETERS AND ROTATIONAL CONSTANTS OF 9-CHLOROANTHRACENE

Thermodynamic parameter	9- Chloro-anthracene
SCF energy (Hartree)	-999.280203
Total energy (thermal) (E_{total}, Kcal mol^{-1})	122.132
Heat capacity at const. Volume (c_v, cal mol^{-1} k^{-1})	44.603
Entropy (S, cal mol^{-1} k^{-1})	101.962
Vibrational energy (E_{vib}, kcal mol^{-1})	120.355
Zero-point vibrational energy (E_0, kcal mol^{-1})	115.39742
Rotational constants (GHz)	
A	0.96181
B	0.45037
C	0.30674

Molecular docking studies: The proteins tyrosinase and HER2 are good-looking targets for the evaluation of anticancer agents [53]. They also play a crucial role in the growth of ductal system of the mammary glands [54]. The 3D crystal structure of protein receptors weretaken from RCSB Protein Data Bank with PDBID: 3PP0, 3NM8 for HER2 and tyrosinase, respectively. The water molecules are eliminated using the UCSF chimera 1.10.1 software. The docking process was executed in between rigid protein receptor and 9-chloroanthracene. Employing ADT program gasteiger, Non-polar hydrogens and torsions degrees of freedom were assigned. The hydrogen bonding interactions between donor and acceptor atoms was fixed to be 1.9 Å. The energy calculations were performed by genetic algorithms [55,56]. A cubic gridbox was also built with dimensions of 60 × 60 × 60 Å^3 on the receptor HER2 and tyrosinase with the aid of AutoDock Tools 1.5.6 program with grid point spacing of 0.3750 Å. The output of the docking

studies of 9-chloroanthracene including binding energies of receptor-ligand complex is illustrated in Table-9 and Fig. 5.

TABLE-9
BINDING ENERGIES OF COMPOUND 9-CHLOROANTHRACENE AGAINST IDO1 RECEPTOR (PDB ID: 3PP0, 3NM8)

Compound	Binding energies (Kcal/mol) PDB ID: 3PP0	Binding energies (Kcal/mol) PDB ID: 3NM8
9-Chloroanthracene	-6.93	-7.39

As shown in Table-9 9-chloroanthracene shows strong binding behaviour against HER2 and tyrosinase with their minimum binding energies of –6.93 and –7.39 kcal mol^{-1}, respectively shows anticancer activity theoretically.

Fukui function analysis: To determine the chemical reactivity and selectivity Fukui function analysis was used. It is local reactivity descriptors that show the propensity of the electronic density to deform at a given position in order to accepting and donating the electrons [57-60]. The condensed Fukui function of nucleophilic, electrophilic and radial attack is calculated by using this equation,

$$f_r^+ = q_r(N+1) - q_r(N) \text{ for nucleophilic attack}$$

$$f_r^- = q_r(N) - q_r(N-1) \text{ for electrophilic attack}$$

$$f_r^0 = 1/2\,[q_r(N+1) - q_r(N-1)] \text{ for radical attack}$$

Fukui function and local softness for 9-chloroanthracene have been listed in Table-10. The lower value of Cl_{24}, shows the accessible site for electrophilic attack. Form Table-10, indicates the reactivity order for electrophilic case as $Cl_{24} > C_4 > H_{17} =$

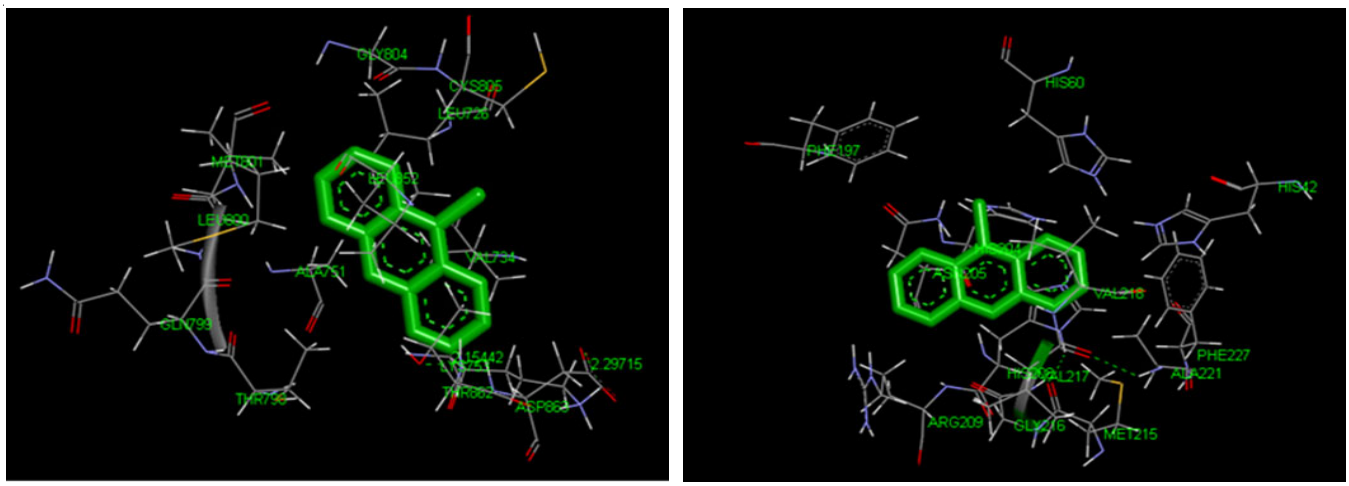

Fig. 5. The binding poses and interactions of 9-chloroanthracene compound to the binding sites of HER2 receptor (top, PDB ID: 3PP0) and tyrosinase receptor (bottom, PDB ID: 3NM8)

TABLE-10
CONDENSED FUKUI FUNCTION (fr) AND NEW DESCRIPTOR (sf)r FOR 9-CHLOROANTHRACENE

Atom	Mulliken atomic charges			Fukui functions			Local softness		
	0, 1 (N)	N + 1 (-1, 2)	N-1 (1, 2)	fr+	fr-	fr0	sr+fr+	sr-fr-	sr0fr0
C1	-1.19132	-1.227558	-1.141155	-0.036239	-0.05016	-0.0432	-0.00758	-0.01049	-0.00903
C2	-0.53622	-0.579851	-0.508971	-0.043631	-0.02725	-0.03544	-0.00912	-0.0057	-0.00741
C3	-0.39584	-0.434717	-0.367274	-0.038874	-0.02857	-0.03372	-0.00813	-0.00597	-0.00705
C4	-0.05377	-0.101113	0.006114	-0.047342	-0.05989	-0.05361	-0.0099	-0.01252	-0.01121
C5	1.270902	1.276276	1.28467	0.005374	-0.01377	-0.0042	0.001124	-0.00288	-0.00088
C6	-0.0541	-0.117546	-0.00229	-0.063451	-0.05181	-0.05763	-0.01327	-0.01083	-0.01205
C7	1.271396	1.276762	1.28518	0.005366	-0.01378	-0.00421	0.001122	-0.00288	-0.00088
C8	-0.05368	-0.101048	0.006227	-0.047373	-0.0599	-0.05364	-0.00991	-0.01253	-0.01122
C9	-0.39562	-0.434453	-0.367066	-0.038831	-0.02856	-0.03369	-0.00812	-0.00597	-0.00705
C10	-0.53628	-0.579959	-0.509014	-0.04368	-0.02727	-0.03547	-0.00913	-0.0057	-0.00742
C11	-1.19188	-1.228105	-1.141722	-0.03623	-0.05015	-0.04319	-0.00758	-0.01049	-0.00903
C12	0.154852	0.164197	0.134241	0.009345	0.020611	0.014978	0.001954	0.00431	0.003132
C13	-0.55866	-0.562226	-0.569237	-0.003568	0.010579	0.003505	-0.00075	0.002212	0.000733
C14	0.154615	0.163978	0.133989	0.009363	0.020626	0.014995	0.001958	0.004313	0.003135
H15	0.160676	0.118608	0.2022	-0.042068	-0.04152	-0.0418	-0.0088	-0.00868	-0.00874
H16	0.177773	0.116993	0.235808	-0.06078	-0.05804	-0.05941	-0.01271	-0.01214	-0.01242
H17	0.162052	0.101202	0.22048	-0.06085	-0.05843	-0.05964	-0.01272	-0.01222	-0.01247
H18	0.14324	0.091323	0.195318	-0.051917	-0.05208	-0.052	-0.01086	-0.01089	-0.01087
H19	0.063181	0.000837	0.123738	-0.062344	-0.06056	-0.06145	-0.01304	-0.01266	-0.01285
H20	0.143236	0.091314	0.195319	-0.051922	-0.05208	-0.052	-0.01086	-0.01089	-0.01087
H21	0.162054	0.1012	0.220486	-0.060854	-0.05843	-0.05964	-0.01272	-0.01222	-0.01247
H22	0.177773	0.116988	0.235809	-0.060785	-0.05804	-0.05941	-0.01271	-0.01214	-0.01242
H23	0.160684	0.118612	0.20221	-0.042072	-0.04153	-0.0418	-0.0088	-0.00868	-0.00874
Cl24	0.764922	0.628285	0.924939	-0.136637	-0.16002	-0.14833	-0.02857	-0.03346	-0.03102

$H_{21} > H_{16} = H_{22}$ and nucleophilic case is C_5 and C_7. These results show 9-chloroanthracene has biological activity.

Atomic natural charges: By using NBO analysis, the atomic natural charges have been determined [61-63] and the results are presented in Fig. 6 and Table-11. The charge distribution of the molecule has an important influence on the vibrational spectra. The charge on the C13 atom attached to chlorine atom is positive compared with all the aromatic carbon of anthracene ring due to electron withdrawing nature of chlorine atom attached to a carbon atom in the title compound. All the remaining charges are reported in Table-11.

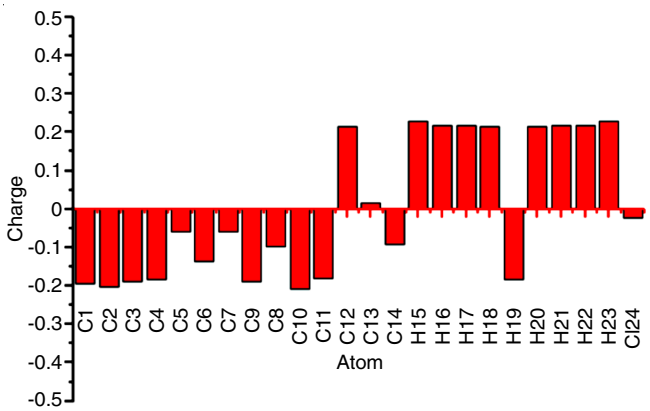

Fig. 6. Mulliken atomic charge of 9-chloroanthracene

TABLE-11
ATOMIC NATURAL CHARGES FOR 9-CHLOROANTHRACENE

Atom	Charge	Atom	Charge
C1	-0.17954	C13	0.01622
C2	-0.20816	C14	-0.09848
C3	-0.18837	H15	0.227994
C4	-0.18250	H16	0.21623
C5	-0.055982	H17	0.21621
C6	-0.13520	H18	0.21577
C7	-0.059889	H19	0.21578
C8	-0.18259	H20	0.21577
C9	-0.18780	H21	0.21617
C10	-0.20126	H22	0.21623
C11	-0.19297	H23	0.22793
C12	-0.09313	H24	-0.02182

Conclusion

In the present study, quantum chemical calculations have been carried on the structure of the molecule under study according to the SQM method using DFT at B3LYP/6-311++G(d,p) level for optimized geometry. The structural parameters obtained in DFT calculations are in good accord with reported single crystal data. All the vibrational frequencies of 9-chloroanthracene observed from FTIR spectra are ascribed on unambiguously employing eigenvectors and PED obtained from DFT. The scaling factors have been refined with an rms error of 8.48 cm^{-1} between the experimental and SQM wave numbers. The study of first-order hyperpolarizability reveals that the molecule exhibits good NLO behaviour. The small HOMO-LUMO energy gap obtained in this molecule indicates that it is more stable and polarizable, exhibit high chemical reactivity and low kinetic stability. The electrophilic, nucleophilic, radial attack within the 9-chloroanthracene was investigated using Fukui function analysis. The MESP of the molecule 9-chloroanthracene was observed that the region around aromatic carbon atoms of anthracene ring has a negative electrostatic potential region and the region around Cl atom has positive electrostatic potential. Which convey that negative potential region is electrophilic and positive region potential region is nucleophilic. Moreover, the molecular docking results reveal that the title molecule exhibits minimum binding energies against HER2 and tyrosinase, which represents the molecule under investigation, shows anticancer activity theoretically.

ACKNOWLEDGEMENTS

The author's thanks to the DST, Government of India (Project code-SB/EMEQ/2014) for providing fellowship.

CONFLICT OF INTEREST

The authors declare that there is no conflict of interests regarding the publication of this article.

REFERENCES

1. M. Saleem, M. Rafiq and M. Hanif, *J. Fluoresc.*, **27**, 31 (2017); https://doi.org/10.1007/s10895-016-1933-x.
2. Y. Jiao, B. Zhu, J. Chen and X. Duan, *Theranostics*, **5**, 173 (2015); https://doi.org/10.7150/thno.9860.
3. Y. Jeong and J. Yoon, *Inorg. Chim. Acta*, **381**, 2 (2012); https://doi.org/10.1016/j.ica.2011.09.011.
4. B. Angelov, A. Angelova and R. Ionov, *J. Phys. Chem. B*, **104**, 9140 (2000); https://doi.org/10.1021/jp993779b.
5. A.P. de Silva, H. Gunaratne, T. Gunnlaugsson and P. Lynch, *New J. Chem.*, **20**, 871 (1996).
6. G.R. Martinez, F. Garcia, L.H. Catalani, J. Cadet, M.C.B. Oliveira, G.E. Ronsein, S. Miyamoto, M.H.G. Medeiros and P.D. Mascio, *Tetrahedron*, **62**, 10762 (2006); https://doi.org/10.1016/j.tet.2006.08.094.
7. L. Yang, Y. Liu, X. Zhou, Y. Wu, C. Ma, W. Liu and C. Zhang, *Dyes Pigments*, **126**, 232 (2016); https://doi.org/10.1016/j.dyepig.2015.11.028.
8. H. Moon, Y.W. Jun, D. Kim, H.G. Ryu, T. Wang, K.H. Kim, Y. Huh, J. Jung and K.H. Ahn, *Chem. Asian J.*, **11**, 2518 (2016); https://doi.org/10.1002/asia.201600986.
9. F.A. Tanious, T.C. Jenkins, S. Neidle and W.D. Wilson, *Biochemistry*, **31**, 11632 (1992); https://doi.org/10.1021/bi00161a050.
10. S.K. Carter, F.M. Schabel Jr., L.E. Broder and T.P. Johnston, *Adv. Cancer Res.*, **16**, 273 (1972).
11. S.A. De Silva, A. Zavaleta, D.E. Baron, O. Allam, E.V. Isidor, N. Kashimura and J.M. Percarpio, *Tetrahedron Lett.*, **38**, 2237 (1997); https://doi.org/10.1016/S0040-4039(97)00332-8.
12. J.W. Sidman, *J. Chem. Phys.*, **25**, 115 (1956); https://doi.org/10.1063/1.1742800.
13. S. Kou, H. Zhou, G. Tang, R. Li, Y. Zhang, J. Zhao and C. Wei, *Spectrochim. Acta A: Mol. Biomol. Spectrosc.*, **96**, 768 (2012); https://doi.org/10.1016/j.saa.2012.07.007.
14. I. Turowska-Tyrk and K. Grzesniak, *Acta Cryst.*, **C60**, o146 (2004); https://doi.org/10.1107/S0108270103026775.
15. M.J. Frisch, G.W. Trucks, H.B. Schlegel, G.E. Scuseria, M.A. Robb, J.R. Cheeseman, G. Scalmani, V. Barone, B. Mennucci, G.A. Petersson, H. Nakatsuji, M. Caricato, X. Li, H.P. Hratchian, A.F. Izmaylov, J. Bloino, G. Zheng, J.L. Sonnenberg, M. Hada, M. Ehara, K. Toyota, R. Fukuda, J. Hasegawa, M. Ishida, T. Nakajima, Y. Honda, O. Kitao, H. Nakai, T. Vreven, J.A. Montgomery Jr., J.E. Peralta, F. Ogliaro, M. Bearpark, J.J. Heyd, E. Brothers, K.N. Kudin, V.N. Staroverov, R. Kobayashi, J. Normand, K. Raghavachari, A. Rendell, J.C. Burant, S.S. Iyengar, J. Tomasi, M. Cossi, N. Rega, J.M. Millam, M. Klene, J.E. Knox, J.B. Cross, V. Bakken, C. Adamo, J. Jaramillo, R. Gomperts, R.E. Stratmann, O. Yazyev, A.J. Austin, R. Cammi, C. Pomelli, J.W. Ochterski, R.L. Martin,

K. Morokuma, V.G. Zakrzewski, G.A. Voth, P. Salvador, J.J. Dannenberg, S. Dapprich, A.D. Daniels, Ö. Farkas, J.B. Foresman, J.V. Ortiz, J. Cioslowski and D.J. Fox, Gaussian Inc.: Wallingford CT (2009).
16. http://autodock.scripps.edu/resources/references.
17. S. Diego, Accelrys Software Inc., Discovery Studio Modeling Environment, Release 4.1.0, Accelrys Software Inc, USA (2013).
18. G. Fogarasi, X. Zhou, P.W. Taylor and P. Pulay, *J. Am. Chem. Soc.*, **114**, 8191 (1992); https://doi.org/10.1021/ja00047a032.
19. G. Fogarasi, P. Pulay and J.R. Durig, Vibrational Spectra and Structure, Elsevier: New York, vol. 14 (1991).
20. T. Sundius, *J. Mol. Struct.*, **218**, 321 (1990); https://doi.org/10.1016/0022-2860(90)80287-T.
21. T. Sundius, *Vib. Spectrosc.*, **29**, 89 (2002); https://doi.org/10.1016/S0924-2031(01)00189-8.
22. P. Pulay, G. Fogarasi, G. Pongor, J.E. Boggs and A. Vargha, *J. Am. Chem. Soc.*, **105**, 7037 (1983); https://doi.org/10.1021/ja00362a005.
23. A. Berces and T. Ziegler, *J. Chem. Phys.*, **98**, 4793 (1993); https://doi.org/10.1063/1.464983.
24. G. Fogarasi, P. Pulay and J.R. Durig, Vibrational Spectra and Structure, Elsevier: Amsterdam, vol. 4 (1985).
25. J.B. Foresman and A. Frisch, Exploring Chemistry with Electronics Structure Methods, Gaussian Inc.: Pittsburg, PA, edn 2 (1996).
26. J. Prashanth, B.V. Reddy and G.R. Rao, *J. Mol. Struct.*, **1117**, 79 (2016); https://doi.org/10.1016/j.molstruc.2016.03.062.
27. J.K. Ojha, B.V. Reddy and G.R. Rao, *Spectrochim. Acta A: Mol. Biomol. Spectrosc.*, **96**, 632 (2012); https://doi.org/10.1016/j.saa.2012.06.035.
28. T. Joseph, H.T. Varghese, C.Y. Panicker, K. Thiemann, K. Viswanathan, C. Van Alsenoy and T.K. Manojkumar, *Spectrochim. Acta A: Mol. Biomol. Spectrosc.*, **117**, 413 (2014); https://doi.org/10.1016/j.saa.2013.08.016.
29. D. Kafer, G. Witte, P. Cyganik, A. Terfort and C. Woll, *J. Am. Chem. Soc.*, **128**, 1723 (2006); https://doi.org/10.1021/ja0571592.
30. P. Pavitha, J. Prashanth, G. Ramu, G. Ramesh, K. Mamatha and B.V. Reddy, *J. Mol. Struct.*, **1147**, 406 (2017); https://doi.org/10.1016/j.molstruc.2017.06.095.
31. J.V. Lockard, A. Butler Ricks, D.T. Co and M.R. Wasielewski, *Phys. Chem. Lett.*, **1**, 215 (2010); https://doi.org/10.1021/jz900136a.
32. M. Kumar, S. Roy, M.S.H. Faizi, S. Kumar, M.K. Singh, S. Kishor, S.C. Peter and R.P. John, *J. Mol. Struct.*, **1128**, 195 (2017); https://doi.org/10.1016/j.molstruc.2016.08.004.
33. S.J.R. Xavier and A. William, *Proc. Indian Natl. Sci. Acad.*, **59A**, 215 (1993).
34. I. Fleming, Frontier Orbitals and Organic Chemical Reactions, John Wiley & Sons: New York (1976).
35. D.F.V. Lewis, C. Ioannides and D.V. Parke, *Xenobiotica*, **24**, 401 (1994); https://doi.org/10.3109/00498259409043243.
36. R.J. Parr, L.V. Szentpaly and S. Liu, *J. Am. Chem. Soc.*, **121**, 1922 (1999); https://doi.org/10.1021/ja983494x.
37. N. Ozdemir, B. Eren, M. Dincer and V. Bekdemir, *Mol. Phys.*, **108**, 13 (2010); https://doi.org/10.1080/00268970903476688.
38. P.N. Prasad and D.J. Williams, Introduction to Nonlinear Optical Effects in Molecules and Polymers, Wiley: New York (1991).
39. F. Meyers, S.R. Marder, B.M. Pierce and J.L. Bredas, *J. Am. Ceram. Soc.*, **116**, 10703 (1994).
40. F. Hinchliffe and R.W. Munn, Molecular Electromagnetism, John Wiley & Sons Ltd.: Chichester (1985).
41. D.A. Kleinman, *Phys. Rev.*, **126**, 1977 (1962); https://doi.org/10.1103/PhysRev.126.1977.
42. R. Zhang, B. Du, G. Sun and Y.X. Sun, *Spectrochim. Acta A: Mol. Biomol. Spectrosc.*, **75**, 1115 (2010); https://doi.org/10.1016/j.saa.2009.12.067.
43. M. Arivazhagan and S. Jeyavijayan, *Spectrochim. Acta A: Mol. Biomol. Spectrosc.*, **79**, 376 (2011); https://doi.org/10.1016/j.saa.2011.03.036.
44. P. Politzer and D.G. Truhlar, Chemical Applications of Atomic and Molecular Elecrostatic Potentials: Reactivity, Structure, Scattering, and Energetics of Organic, Inorganic and Biological Systems, Plenum Press: New York (1981).
45. E. Scrocco and J. Tomasi, *J. Adv. Quantum Chem.*, **11**, 115 (1978); https://doi.org/10.1016/S0065-3276(08)60236-1.
46. P. Politzer and K.C. Daiker, ed.: B.M. Deb, Models for chemical reactivity, In: The Force Concept in Chemistry, Van Nostrand Reinhold: New York (1981).
47. V. Balachandran and V. Karunakaran, *Spectrochim. Acta A: Mol. Biomol. Spectrosc.*, **106**, 284 (2013); https://doi.org/10.1016/j.saa.2012.12.070.
48. L. Rajith, A.K. Jissy, K.G. Kumar and A. Datta, *J. Phys. Chem. C*, **115**, 21858 (2011); https://doi.org/10.1021/jp208027s.
49. E.D. Glendening, A.E. Reed, J.E. Carpenter and F. Weinhold, NBO Version 3.1, TCI, University of Wisconsin: Madison (1998).
50. S. Sebastian and N. Sundaraganesan, *Spectrochim. Acta A: Mol. Biomol. Spectrosc.*, **75**, 941 (2010); https://doi.org/10.1016/j.saa.2009.11.030.
51. G. Herzberg, Infrared and Raman Spectra of Polyatomic Molecules, D. Van Nostrand: New York (1945).
52. K.S. Pitzer and W.D. Gwinn, *J. Chem. Phys.*, **10**, 428 (1942); https://doi.org/10.1063/1.1723744.
53. R. Konakanchi, J. Haribabu, J. Prashanth, V.B. Nishtala, R. Mallela, S. Manchala, D. Gandamalla, R. Karvembu, B.V. Reddy, N.R. Yellu and L.R. Kotha, *Appl. Organomet. Chem.*, **32**, e4415 (2018); https://doi.org/10.1002/aoc.4415.
54. R.S. Herbst, *Int. J. Radiat. Oncol. Biol. Phys.*, **59**, S21 (2004); https://doi.org/10.1016/j.ijrobp.2003.11.041.
55. J. Sebastian, R.G. Richards, M.P. Walker, J.F. Wiesen, Z. Werb, R. Derynck, Y.K. Hom, G.R. Cunha and R.P. Di Augustine, *Cell Growth Differ.*, **9**, 777 (1998).
56. R. Konakanchi, R. Mallela, R. Guda and L.R. Kotha, *Res. Chem. Intermed.*, **44**, 27 (2017); https://doi.org/10.1007/s11164-017-3089-y.
57. R. Mallela, R. Konakanchi, R. Guda, N. Munirathinam, D. Gandamalla, N.R. Yellu and L.R. Kotha, *Inorg. Chim. Acta*, **469**, 66 (2018); https://doi.org/10.1016/j.ica.2017.08.042.
58. R.G. Parr and W. Yang, Functional Theory of Atoms and Molecules, Oxford University Press: New York (1989).
59. P.W. Ayers and R.G. Parr, *J. Am. Chem. Soc.*, **122**, 2010 (2000); https://doi.org/10.1021/ja9924039.
60. R.G. Parr and W.J. Yang, *J. Am. Chem. Soc.*, **106**, 4049 (1984); https://doi.org/10.1021/ja00326a036.
61. P.K. Chattaraj, B. Maiti and U. Sarkar, *J. Phys. Chem. A*, **107**, 4973 (2003); https://doi.org/10.1021/jp034707u.
62. T.J. Beaula, I.H. Joe, V.K. Rastogi and V.B. Jothy, *Chem. Phys. Lett.*, **624**, 93 (2015); https://doi.org/10.1016/j.cplett.2015.02.026.
63. C.S. Abraham, J.C. Prasana and S. Muthu, *Spectrochim. Acta A: Mol. Biomol. Spectrosc.*, **181**, 153 (2017); https://doi.org/10.1016/j.saa.2017.03.045.